ELSEVIER

Chemical Engineering Journal 82 (2001) 183–188

Chemical Engineering Journal

www.elsevier.com/locate/cej

Ultrafine particle fluidization and its application to photocatalytic NO_x treatment

Satoru Matsuda [a,*], Hiroyuki Hatano [a], Atsushi Tsutsumi [b]

[a] *National Institute for Resources and Environment, 16-3 Onogawa, Tsukuba 305-8569, Japan*
[b] *The University of Tokyo, 7-3-1 Hongo Bunkyo-ku, Tokyo 113-8656, Japan*

Received 29 May 2000; accepted 13 October 2000

Abstract

The fluidized bed of ultrafine particle of photocatalyst is applied to treat nitrogen oxides (NO_x) by photocatalytic oxidation. Three different TiO_2 particles with primary particle diameters of 7, 20 and 200 nm are used as the bed material. The removal of NO_x using a two-dimensional fluidized bed of ultrafine TiO_2 particles is investigated. The fluidized bed of 7 nm TiO_2 exhibits high removal efficiency of NO_x because of its large specific surface area. It is found that the amount of NO_x removal is proportional to the specific surface area. The fluidization of three kinds of photocatalysts shows the following characteristics. Agglomerates of 7 and 20 nm particles appear to be so hard that they are not destroyed during fluidization because of large adhesion forces of particles. In the case of 7 and 20 nm particle systems, the bed height is found to increase progressively with the increase in gas velocity, while the bed expansion is observed to level off for 200 nm particle system. The entrainment rate of 7 and 20 nm particle systems is found to be smaller than that of 200 nm particle system.

Keywords: Ultrafine particle; Nanoparticle; Agglomerate; Photocatalyst; NO_x

1. Introduction

In spite of the stringent emission control regulations and the massive installation of emission reduction systems, the air pollution of nitrogen oxides (NO_x) becomes a serious problem in Japan [2]. The increase in the number of automobiles and limited traffic capacity deteriorate the pollution of NO_x especially in the urban area. Ibusuki and Takeuchi [3,4,13] have reported that some semiconductor metal oxides can adsorb and transform photochemically NO_x into nitric acid. Titanium dioxide, in particular, is suitable for photocatalyst of NO_x treatment because of its high efficiency, chemical stability, harmlessness and cheapness. They proposed the sheet-like photocatalyst mixed with an adsorbent which is setup on the sidewall of the road [10,14,15]. This is a passive method to reduce the NO_x level in the atmosphere without external operation, which has been already adopted as practical NO_x treatment in several large cities in Japan. It is difficult, however, for sheet-like photocatalyst to treat large amount of gas such as tunnel exhaust continuously. The photocatalytic reaction occurs only on the surface of photocatalyst particle, leading to the necessity of large space with illuminated surface. Moreover, the nitric acid formed on the surface of catalyst must be taken off to maintain the photocatalytic activity.

Authors [7,8] proposed the photocatalytic NO_x removal system using fluidization technology to treat large amount of polluted gas. The photocatalyst particles in the fluidized bed reactor are easily charged and discharged, resulting in the construction of continuous NO_x treatment system with additional regeneration process of photocatalyst. The regeneration of photocatalyst can be achieved by heating to take off the nitric acid. In the photocatalytic oxidation of NO_x, the reaction rate is influenced by the gas–solid contacting and the irradiation efficiency of ultraviolet (UV) light. The motions of photocatalyst particles in the fluidized bed induce large mass transfer rate in the whole bed and effective renewal of illuminated surface of photocatalyst. Therefore, the efficient removal of NO_x from the exhaust can be expected in the photocatalytic NO_x treatment using the fluidized bed of photocatalyst particles. In the previous work [8], photocatalyst with primary particle diameter of 20 nm was achieved to be fluidized and remove NO_x. It was found that operating conditions such as light intensity, gas velocity and bed height have positive influences on the NO_x treatment process. Especially, the sufficient irradiation of UV light was found to be attained to penetrate

* Corresponding author. Tel.: +81-298-61-8226; fax: +81-298-61-8209.
E-mail address: matsuda@nire.go.jp (S. Matsuda).

1385-8947/01/$ – see front matter
PII: S1385-8947(00)00339-9

Nomenclature

C_{NO_x}	concentration of nitrogen oxides (NO and NO_2) (ppm)
d_p	particle diameter (m)
H	dense bed height (m)
H_c	settled bed height (m)
H_{init}	settled bed height at initial setup (m)
I	normalized lightness of digitized image at local point (–)
L_d	distance from distributor (m)
M	cumulative removed NO_x (mol/g)
S_w	specific surface area (m^2/g)
t	time (s)
u_0	superficial gas velocity (m/s)
ρ_b	bulk density (g/m^3)

whole of the fluidized bed reactor even if the large size of bed.

The amount of NO_x removal is thought to be dependent on the specific surface area of photocatalyst. Thus, ultrafine particle is preferable in the photocatalytic NO_x treatment. The fluidized bed of ultrafine particles is recently receiving much attention with the increasing potential of wide application. Chaouki et al. [1] found that the CuO/Al_2O_3 aerogels are smoothly fluidized if the gas velocity is increased far above the minimum fluidization velocity of primary particles. Morooka et al. [9] investigated the fluidization of submicron particles such as Ni, Si_3N_4, SiC, Al_2O_3 and TiO_2 and observed that various submicron particles are smoothly fluidized with forming agglomerates. They found that the apparent minimum fluidization velocity and the size of agglomerates are dependent on types of particles and fluidizing gas. As for adhesion force of fine particle, Smolders and Baeyens [12] and Santana et al. [11] reported that the entrainment rate is reduced by interparticle adhesion forces. Several models of fine particle fluidization have been proposed to elucidate the agglomeration of fine particles [1,5,9,16,17]. However, few studies have so far been made at the fluidization of nanoparticles.

In the present paper, the photocatalytic oxidation of NO_x is discussed in the fluidized bed system. The fluidization of three kinds of photocatalysts (d_p: 7, 20 and 200 nm) is investigated for NO_x treatment.

2. Experimental

2.1. Experimental apparatus

Fig. 1 shows the experimental apparatus. The flow rate of air from a compressor and NO standard gas is controlled by mass flow controllers to adjust the NO_x level. Both of gases are mixed in a gas blender (GB-4C, KOFLOC). The gas is introduced into a two-dimensional fluidized bed reactor with 2 mm × 70 mm cross-section. The glass beads of 1 mm are used as the distributor. The wall is made of pyrex-glass (2 mm in thickness). The expanding section (230 mm in height, 50 mm × 70 mm cross-section at the top) is installed on the reactor to decrease the amount of carryover particles. The reactor is illuminated with UV light sources (FL15BL, 2 × 15 W, TOSHIBA) in a dark box. The intensity of UV light is measured by digital radiometer (DRC-100, DIX-365 sensor, SPECTROLINE). The UV light intensity at the surface of light sources is 1.94 mW/cm^2. The intensities of UV light transmitted through the bed vary from 0.40 to 0.90 mW/cm^2 according to the bed density. The concentration of NO_x (C_{NO_x}) is continuously measured by a chemiluminescence-type analyzer (NOA-7000, SHIMAZU). The signals from the analyzer are transferred to a computer after A/D converted by a data logger (Thermodac-E, ETODENKI) and are recorded as time series data.

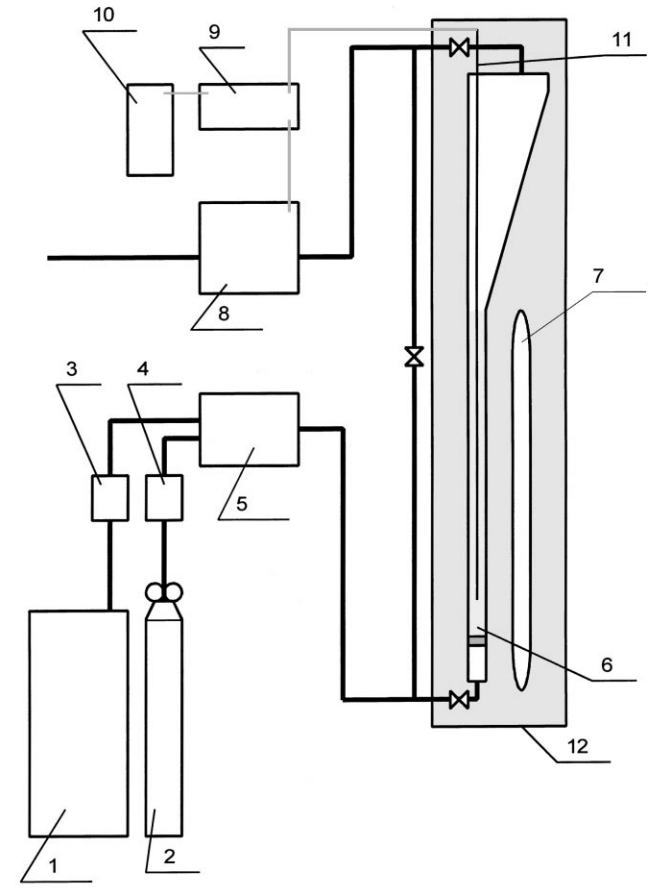

Fig. 1. Experimental apparatus.

Table 1
Specification of particles

Particle	Component	d_p (nm)	S_w (m^2/g)	ρ_b (kg/m^3)
1	TiO_2 (anatase)	7	334.0	300
2	TiO_2 (anatase)	20	63.8	460
3	TiO_2 (anatase)	200	9.2	340

2.2. Visual observation

A CCD video camera is used for flow visualization. The shutter speed of camera is 0.1 ms. The images are recorded on 8 mm videotapes and are converted to digitized images of 640 × 480 pixels through the video-capturing device of the PC.

2.3. Density distribution of agglomerates

The local lightness of digitized images is measured for estimation of the density distribution of agglomerates. The lightness of particulate phase and background without fluidization are assumed as 1 and 0.

2.4. Photocatalyst

Table 1 shows the specification of photocatalyst used in this work (ST-series, Ishihara Techno Corp.). The amount of photocatalyst put on the reactor is 0.5 g for all cases. The mechanism of NO_x oxidation by photocatalyst (TiO_2) is as follows [3,6]. TiO_2 generates the positive holes (h^+) and photoelectrons (e^-) on the surface under illumination of UV light (300–400 nm). The hydrogen ions (H^+) and hydroxide ions (OH^-) are dissociated from H_2O.

$$H_2O \rightarrow H^+ + OH^- \quad (1)$$

The active oxygen species are produced on the TiO_2 surface.

$$e^- + O_2 \rightarrow O_2^- \quad (2)$$

$$h^+ + OH^- \rightarrow OH^* \quad (3)$$

$$H^+ + O_2^- \rightarrow HO_2^* \quad (4)$$

The nitric oxides (NO_x) are oxidized to nitric acid (HNO_3) by active oxygen species.

$$NO + HO_2^* \rightarrow NO_2 + OH^* \quad (5)$$

$$NO_2 + OH^* \rightarrow HNO_3 \quad (6)$$

Finally, the nitric acid forms on catalyst. The activity of photocatalyst loses with accumulation of HNO_3.

2.5. Experimental procedure

At the beginning of gas injection, channeling and/or partial fluidization often take place. By tapping with hands, gas jet is developed in the region of no fluidization and fine particles agglomerate, leading to smooth fluidization of the whole bed. When once agglomerates of ultrafine particles formed, normal fluidization is achieved without the addition of external energy.

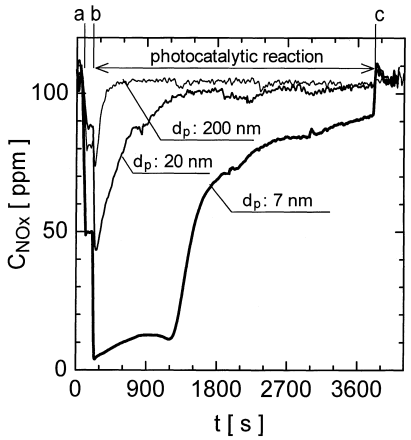

Fig. 2. NO_x conversion profiles in ultrafine particle fluidized bed (u_0: 23.4 cm/s).

3. Results and discussion

Fig. 2 shows NO_x conversion profiles in the fluidized bed. Introducing NO_x gas of 100 ppm with air balance into the fluidized bed reactor of ultrafine photocatalyst, the NO_x concentration in the outlet decrease initially with time and level off because of NO_x adsorption on the photocatalyst (point a). When the bed is irradiated with UV light, the photocatalytic NO_x oxidation take place to produce nitric acid, leading to a rapid reduction of NO_x concentration in the outlet (point b). Subsequently, the NO_x concentration in the outlet returns rapidly with time for 20 and 200 nm particle systems. In the case of 7 nm particle, the NO_x concentration in the outlet increase gradually after the photocatalyst exhibited steady reacting for 1000 s. The decrease in photocatalytic activity of the catalysts is due to the coverage of the catalyst surface by HNO_3 formed [10,15]. Finally, the photocatalytic reaction is terminated by turning off the UV light sources (point c), and then the NO_x concentration return to the inlet concentration.

Fig. 3 shows the relationship between specific surface area and the total amount of NO_x removed per unit weight of catalyst in the bed. The amount of NO_x treatment is found to be almost proportional to the specific surface area. This result indicates that the photocatalytic oxidation of NO_x on the surface of particles is the rate-determining step in the NO_x treatment using the ultrafine particle fluidized bed.

In fluidization, agglomerates are formed and may affect the NO_x removal. Fig. 4 shows the snapshots of agglomerates near the distributor. The majority of 7 and 20 nm particles are found to form agglomerates with smooth surface

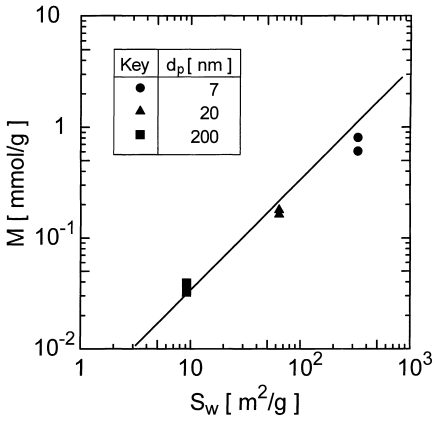

Fig. 3. Relationship between specific surface area and total amount of NO_x removed per unit weight of catalyst in bed.

(Fig. 4a and b). Agglomerates of 7 and 20 nm particles appear to be so hard that they are not destroyed during fluidization. On the other hand, in the case of 200 nm particle (Fig. 4c) the agglomerates are observed to have rough surface and break down into small fragments, forming a defluidization region. These results are attributable to the difference in the strength of the adhesion force of particles. The 200 nm particles are considered to agglomerate into a comparatively weakly linked cluster because of weak interparticle forces. Thus, if the agglomerate of 200 nm particles is sheared in the fluidization, the destruction of agglomerates takes place, resulting in a partial fluidization.

Fig. 5 shows representative snapshots of fluidization of ultrafine particles. In any cases, the formation of dense phase bed is observed with uneven bed surface. As the gas velocity increase, the upper bed surface exhibits more vigorous motion and become obscure. While the bubbles in a conventional fluidized bed of large particles have spherical cap shape, the shape of bubble is observed to be indistinct in the ultrafine particle fluidized bed.

Fig. 6 shows the relationship between bed expansion and superficial gas velocity, u_0. The bed expansion is observed to take place when the gas velocities exceed about 3, 5 and 5 cm/s for 7, 20 and 200 nm particle systems, respectively. In the case of 7 and 20 nm particle systems, the bed height is found to increase progressively with the increase in gas velocity. For 7 nm particle system the bed height is observed to reach a maximum at 18 cm/s and subsequently drop, leading to the extensive elutriation. As can be seen in Fig. 5c, a considerable amount of agglomerates is observed to be distributed homogeneously in the entire freeboard at 23.4 cm/s. On the other hand, for 200 nm particle system the bed expansion is observed to level off above 21 cm/s.

Fig. 7 shows the local lightness in the freeboard and the dense bed regions. This is closely related to the density distribution of agglomerates. It is found that agglomerates homogeneously distribute along the freeboard region. In the case of 7 nm particle system, the elutriation of agglomerate

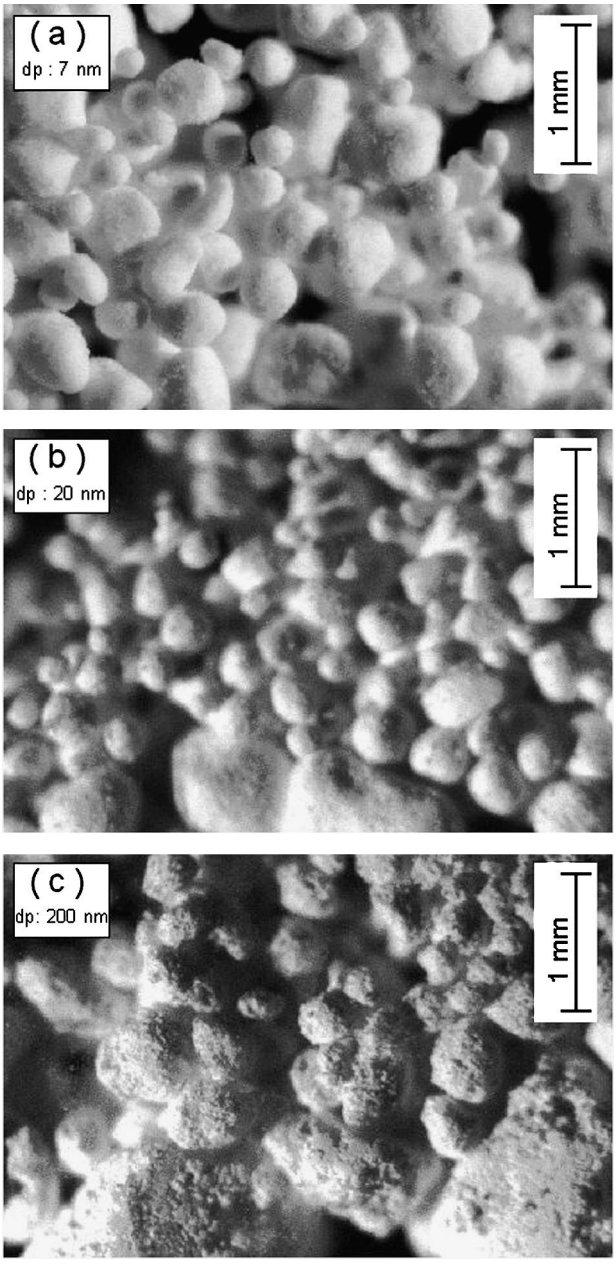

Fig. 4. Local images of fluidization of ultrafine particles near distributor (u_0: 23.4 cm/s; (a) 7 nm; (b) 20 nm; (c) 200 nm).

become significant and the hold-up of agglomerates in the freeboard region increase with increasing gas velocity. On the other hand, in the case of 20 and 200 nm particle systems, the hold-up of agglomerates in the freeboard region is relative small at the same superficial gas velocity.

Fig. 8 shows the typical time courses of the ratio of the settled bed height to the initial settled bed height at the gas velocity of 23.4 cm/s. It represents the amount of remained particles in bed. The gas leaving carries some particles out of the bed. The entrainment rate of 200 nm particle system is found to be larger than that of 7 and 20 nm particle systems. For 200 nm particle, a considerable amounts of

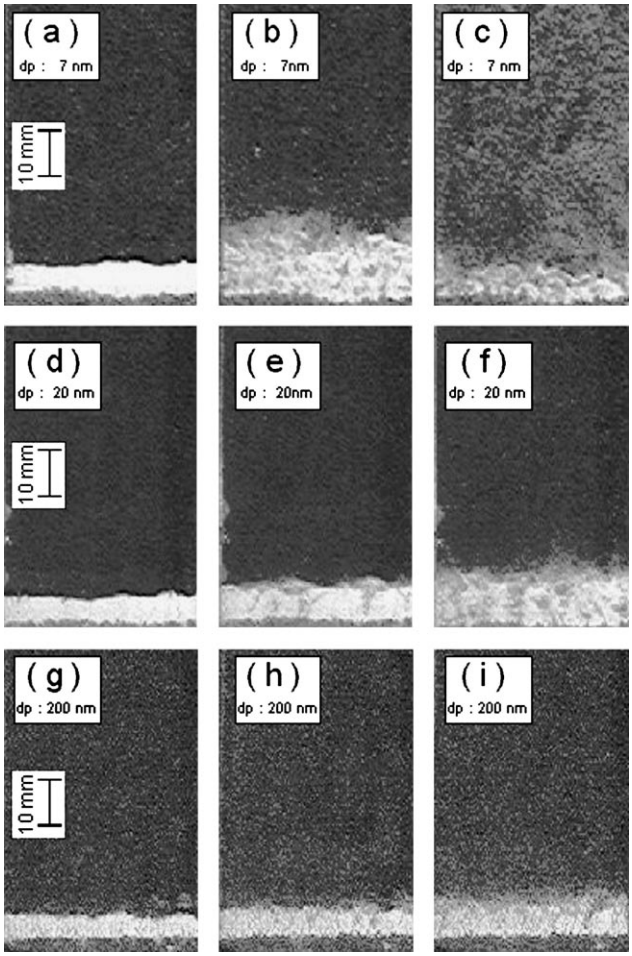

Fig. 5. Representative snapshots of fluidization of ultrafine particles. Weight of particles introduced is 0.5 g for all cases. Superficial gas velocities u_0 are 2.6, 13.0 and 23.4 cm/s from left to right, respectively ((a–c) 7 nm; (d–f) 20 nm; (g–i) 200 nm).

particles carry out of the bed in the initial stage of fluidization. These results indicate that the bed of 200 nm particle contains a larger amount of fine particles whose terminal velocities are much lower than the superficial gas velocity.

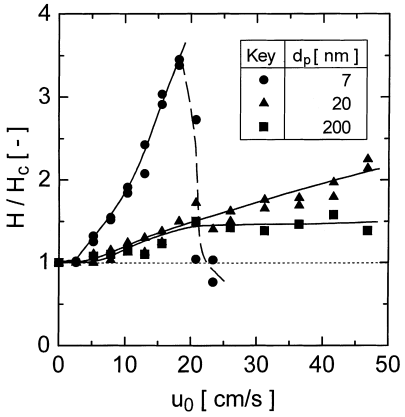

Fig. 6. Relationship between bed expansion and superficial gas velocity.

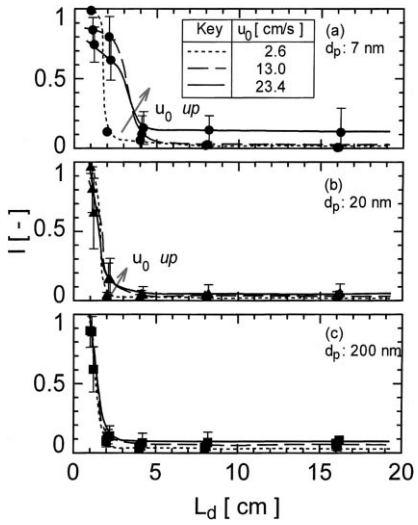

Fig. 7. Local lightness of digitized images. Bars in figure represent maximum and minimum values ((a) 7 nm; (b) 20 nm; (c) 200 nm).

It can be concluded that in the case of 200 nm particle system very fine particles and/or agglomerates are generated by the breakdown of agglomerates during fluidization because of their weaker interparticle forces. On the other hand, the adhesion forces of 7 and 20 nm particles are so strong that most agglomerates are not destroyed, resulting in smaller amount of carryover particles. Similar phenomena were reported in the previous works given by Smolders and Baeyens [12] and Santana et al. [11]. Both of them concluded that the entrainment rate is strongly reduced by interparticle adhesion forces. The conceptual model of ultrafine particle fluidization is summarized in Fig. 9. The specific surface area of each particle is dominant for the amount of NO_x treatment as can be seen in Fig. 3. The fluidization of agglomerates, however, is different each other. These results indicate that the photocatalytic reaction takes place on the surface of primary particle independent of agglomerates structure of each particle in this fluidized bed system. The gas stream

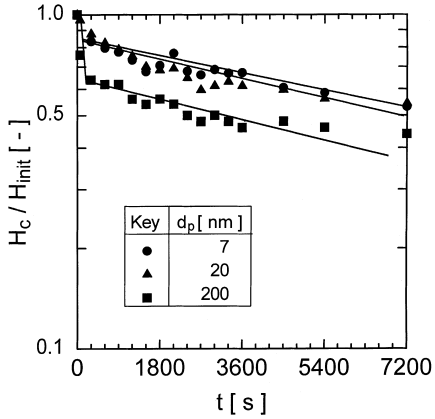

Fig. 8. Typical time courses of amount of remained particles in bed (u_0: 23.4 cm/s).

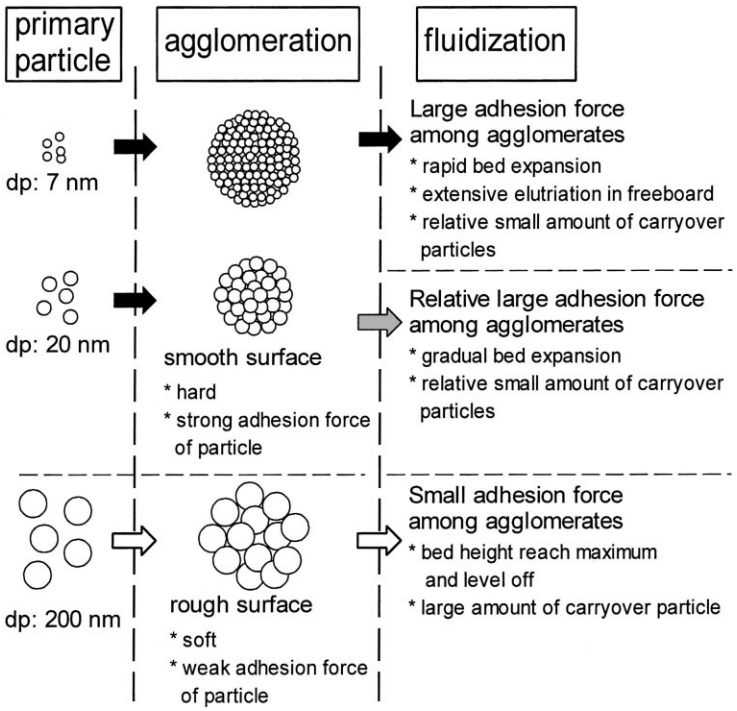

Fig. 9. Conceptual model of ultrafine particle fluidization.

and light irradiation penetrate into agglomerates, resulting in the effective utilization of primary particle as photocatalyst. However, not all primary particles are used as photocatalyst because of the difficulty in penetration into deep inside of agglomerates. Future investigation will be conducted to improve the efficiency of particle utilization.

4. Conclusions

The ultrafine particle fluidized beds of TiO_2 with the primary particle sizes of 7, 20 and 200 nm are applied to treat NO_x by photocatalytic reaction. The removal of NO_x using a two-dimensional fluidized bed of ultrafine TiO_2 photocatalyst is carried out. The hydrodynamic behavior of ultrafine particle fluidization is also conducted. For each particle, the smooth fluidization is achieved with forming agglomerates in the fluidized bed. In the case of nanoparticle system, the photocatalyst exhibit steady reacting for 1000 s. The amount of NO_x treatment is found to be almost proportional to the specific surface area, indicating that the photocatalytic oxidation of NO_x on the surface of particles is the rate-determining step in the NO_x removal mechanism. Agglomerates of 7 and 20 nm particles appear to be so hard that they are not destroyed during fluidization because of large adhesion forces of particles. On the other hand, in the case of 200 nm particle the agglomerates are observed to break down into small fragments. Different ultrafine particles exhibit different fluidization behavior such as the bed expansion, the density distributions of agglomerates and the amount of carryover particles.

Acknowledgments

The authors are grateful to Ishihara Techno Co., Ltd. who provides the photocatalyst particles used in this work.

References

[1] J. Chaouki, C. Chavarie, D. Klvana, G. Pajonk, Powder Technol. 43 (1985) 117–125.
[2] Environmental Agency of Japan, Quality of the Environment in Japan 1994, 1996.
[3] T. Ibusuki, K. Takeuchi, Atmos. Environ. 20 (1986) 1711–1715.
[4] T. Ibusuki, K. Takeuchi, J. Mol. Catal. 88 (1994) 93–102.
[5] Y. Iwadare, M. Horio, Powder Technol. 100 (1998) 223–236.
[6] Y. Komazaki, H. Shimizu, S. Tanaka, Atmos. Environ. 33 (1999) 4363–4371.
[7] S. Matsuda, H. Hatano, Proceedings of the 28th Society of Chemical Engineering Japan Autumn Meeting, Japan (1995) C105.
[8] S. Matsuda, H. Hatano, K. Tsuchiya, Proc. Fluidization IX (1998) 701–708.
[9] S. Morooka, K. Kusakabe, A. Kobata, Y. Kato, J. Chem. Eng. Jpn. 21 (1988) 41–46.
[10] N. Negishi, K. Takeuchi, T. Ibusuki, Appl. Surf. Sci. 121/122 (1997) 417–420.
[11] D. Santana, J.M. Rodriguez, A. Macias-Machin, Powder Technol. 106 (1999) 110–118.
[12] K. Smolders, J. Baeyens, Powder Technol. 92 (1997) 35–46.
[13] K. Takeuchi, T. Ibusuki, Atmos. Environ. 20 (1986) 1155–1160.
[14] K. Takeuchi, K. Toyose, S. Kutsuna, T. Ibusuki, Sigen to Kankyo 3 (1994) 39–46.
[15] K. Takeuchi, N. Negishi, S. Kutsuna, T. Ibusuki, Material Solutions for Environmental Problems, 1997, pp. 161–169.
[16] T. Zhou, H. Li, Powder Technol. 101 (1999) 57–62.
[17] T. Zhou, H. Li, Powder Technol. 111 (2000) 60–65.